有机化学 DOI: 10.6023/cjoc202309026 研究论文
Chinese Journal of Organic Chemistry ARTICLE

一种 Y 型噻吨酮–咔唑分子的设计、合成及其蓝光和黄光有机发光二极管应用

孙 静*,[a,b] 樊志杰[a] 杜纪宽[a] 李 硕[a]
苗艳勤*,[a,b] 赵 波[a] 董海亮[a,b] 王 华*,[a]
([a]太原理工大学 新材料界面科学与工程教育部重点实验室 太原 030024)
([b]山西浙大新材料与化工研究院 太原 030024)

摘要 采用噻吨酮作为受体, 9,9'-(1,3-苯基)二-9*H*-咔唑作为给体, 设计合成了一种 Y 型分子, 命名为 **TX-Ph2Cz**. 化合物在稀释的溶液中展示了位于 420 nm 处的蓝光发射, 且其发射峰在不同极性的溶剂中基本不变. 在四氢呋喃/水的混合溶剂中, 随着含水量的增加发射峰红移了 36 nm. 从其单晶结构中可以看出化合物具有很多分子间相互作用, 分子间的 π···π 作用有助于实现分子间的电荷转移. 化合物 **TX-Ph2Cz** 在掺杂器件(质量分数 3%)中展示了位于 440 nm 的蓝光峰, 而在非掺杂器件中则展示了位于 540 nm 处的黄光峰, 这是因为在薄膜中化合物自身形成了电致激基缔合物. 同时, 非掺杂器件展示了更好的电致发光性能, 最大电流效率和最大外量子效率分别达到 4.91 cd/A 和 2.64%.

关键词 有机发光二极管(OLED); 噻吨酮–咔唑; Y 型结构; 激基缔合物

Design and Synthesis of a Y-Type Thioxanthone-Carbazole for the Application in Blue and Yellow Organic Light-Emitting Diodes

Sun, Jing*,[a,b] Fan, Zhijie[a] Du, Jikuan[a] Li, Shuo[a] Miao, Yanqin*,[a,b]
Zhao, Bo[a] Dong, Hailiang[a,b] Wang, Hua*,[a]
([a] *Key Laboratory of Interface Science and Engineering in Advanced Materials*, *Ministry of Education*, *Taiyuan University of Technology*, *Taiyuan 030024*)
([b] *Shanxi-Zheda Institute of Advanced Materials and Chemical Engineering*, *Taiyuan*, *030024*)

Abstract A Y-shaped emitter, **TX-Ph2Cz**, was designed and synthesized, which uses a thioketone unit as the acceptor and 9,9'-(1,3-phenylene)bis-9*H*-carbazole as the donor. The compound exhibited blue emission at about 420 nm in diluted solution and a small change in the different solvents with various polarities. In the mixed tetrahydrofuran (THF)/H_2O solvents, emission bands had a red shift of 36 nm with the increased content of water. According to the single crystal structure, **TX-Ph2Cz** showed many intermolecular interaction and the π···π interaction between adjacent molecules would increase the intermolecular charge transfer. Critically, **TX-Ph2Cz** exhibited blue emission (440 nm) in the doped device, but yellow emission (540 nm) in the non-doped device was originated from the excimer of **TX-Ph2Cz**. Moreover, the maximum current efficiency and external quantum efficiency of non-doped device were 4.91 cd/A and 2.64%, respectively.

Keywords organic light-emitting diode (OLED); thioxanthone-carbazole derivatives; Y-type structure; excimer

1 Introduction

High-quality luminescent materials have received tremendous attention due to the advantages of easy modification, low cost, high efficiency and environmentally friendly, which exhibit great application prospect in the organic light-emitting diodes (OLEDs), data security protection and bioimaging. Particularly, emitters with donor-acceptor (D-A) structure were the most anticipated that have been developed rapidly and the internal quantum efficiency the-

* Corresponding authors. E-mail: sunjing@tyut.edu.cn; miaoyanqin@tyut.edu.cn; wanghua001@tyut.edu.cn
Received September 27, 2023; revised November 15, 2023; published online December 28, 2023.
Project supported by the National Natural Science Foundation of China (Nos. 62074109, 6207031407), the Joint Funds of the National Natural Science Foundation of China (No. U21A20492), and the Science and Technology Innovation Talent Team Project of Shanxi Province (No. 202204051001013).
国家自然科学基金(Nos. 62074109, 6207031407)、国家自然科学基金委联合基金(No. U21A20492)和山西省科技创新人才队伍建设(No. 202204051001013)资助项目.

oretically achieved 100% through effective reverse intersystem crossing.[1-4] However, it is still a great challenge to establish the relationship between structure and performance. Nowadays, novel design strategies were proposed to optimize and improve the photophysical properties. The general methods were to modulate the electron donating ability of donor, electron withdrawing ability of acceptor, substituent positions and so on. Through rational structural optimization, excellent electroluminescent (EL) performance was achieved.[5-8] It is also found that in the D-A emitters there is not only intramolecular charge transfer (intra-CT) but also intermolecular charge transfer (inter-CT) that was generally called as exciplex. It has already been proved that inter-CT in the linear D-A emitters would perfect the electronic structure and improve the luminous efficiency.[9-10] However, the exciplex materials with inter-CT were usually reported in the doped systems[11-13] that exhibited monochromatic light or white light emission. Regrettably, it was difficult to prepare the high-quality OLEDs based on these materials owing to the multilayer device structure, phase separation and high cost. Therefore, it was very important to develop the high-quality inter-CT emitters between the molecules themselves, especially the configurations of D-A structure.

Recently, different conjugated or flexible spacers were introduced to optimize the charge transfer process in some D-A emitters and new-type luminous mechanism was proposed.[14-16] The above spacer has changed the steric configuration and considerable inter-CT was dominated because of the strong intermolecular interaction. In 2022, Su's group[17] adopted a non-conjugated planar spacer to connect the donor and acceptor that the intermolecular distance was shortened and strong intermolecular interaction was obtained. Owing to the appearance of inter-CT, the compound exhibited a maximum external quantum efficiency (EQE_{max}) of 21.9%.[17] In 2023, Yang and his co-workers[18] reported a hybrid local and charge-transfer (HLCT) material (TRZ-TPM) by optimizing the distance between the donor and acceptor. It exhibited blue emission with an EQE_{max} of 2.5% in the doped device and an 84 nm red-shift with an EQE_{max} of 1.9% in the non-doped device due to the formation of excimer. Based on this, it is confirmed that inter-CT was important for twisted D-A molecules and EL performance would be perfected, such as the light color and luminous efficiency.[19-20]

In this work, we chose π-conjugated thioxanthone units as the acceptor and 9,9'-(1,3-phenylene)bis-9*H*-carbazole as the donor to construct the Y-type emitter (**TX-Ph2Cz**). Owing to the rigid conjugated structure, **TX-Ph2Cz** would have large steric hindrance and the dipole moment in the excited state would be influenced by aggregation. On this basis, intermolecular interaction enhanced and inter-CT state could dominate, providing another radiative transition channel to use the excitons. According to our assumptions, **TX-Ph2Cz** exhibits excellent electroluminescent properties with an excellent excimer emission (540 nm) with an EQE_{max} of 2.64%.

2 Results and discussion

2.1 Molecular synthesis and characterization

In order to design the Y-typed emitter, we firstly chose two carbazole groups as the donors and thioxanthone units as the acceptors, and then the above functional units were connected to the 1-, 3- and 5-positions of benzene. Owing to the asymmetrical Y-typed structure, charge transfer process from the donor to the acceptor would be affected in the process of aggregation. In addition, all intermediates and final product were synthesized by nucleophilic substitution, cyclization and Suzuki coupled reaction that had considerable synthetic yields and simple purification process. The structures of intermediates were confirmed by ^1H

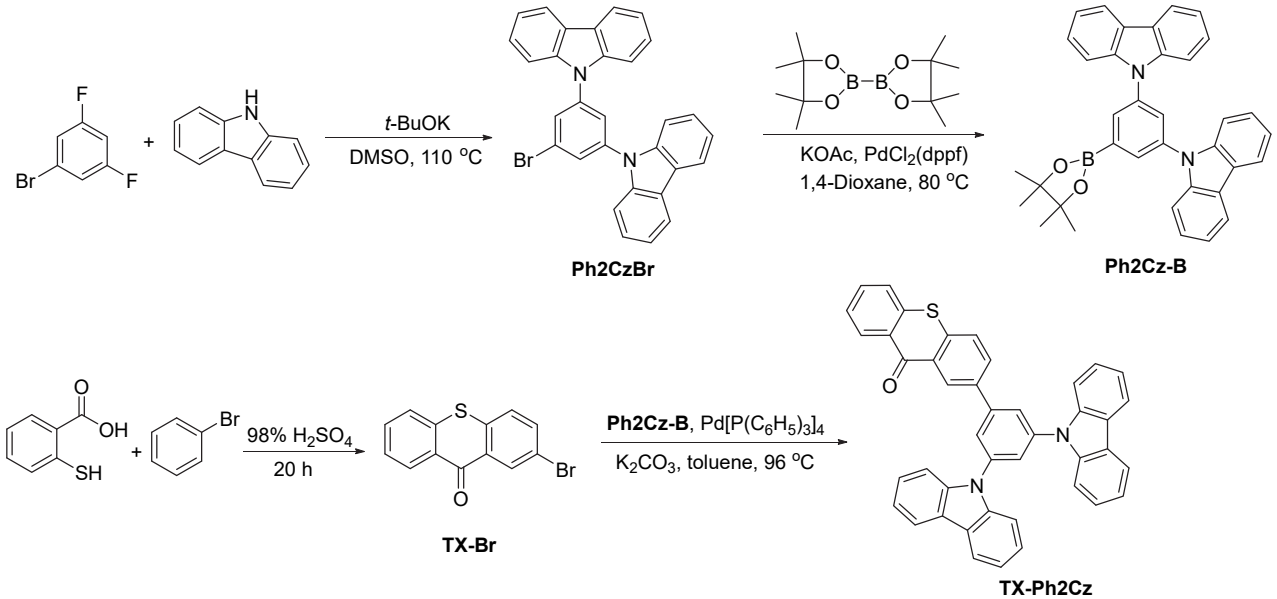

Scheme 1 Synthesis route of the intermediates and **TX-Ph2Cz**

NMR spectra and references, and the final product was confirmed by ^{1}H NMR, ^{13}C NMR, high-resolution mass spectra (HRMS) and elemental analysis. Moreover, the final product exhibited good solubility in the different solvents.

2.2 Thermal stability

Thermogravimetric analysis (TGA) and differential scanning calorimetry (DSC) curves were used to study the thermal stability of **TX-Ph2Cz**. As shown in Figure 1, the decomposition temperature (T_d, corresponding to 5% weight loss) is 383 ℃ and the glass transition temperature (T_g) is 142 ℃. It indicates that the thermal stability of **TX-Ph2Cz** meets the requirements of forming good and stable morphology in the preparation of OLED devices.

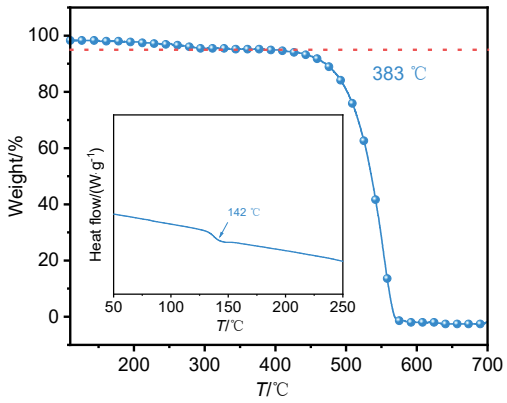

Figure 1 TGA curve and DSC curve of **TX-Ph2Cz**

2.3 Electrochemical property

Cyclic voltammetry (CV) curve using the ferrocene (Fc) as an internal standard was carried out to explore the electrochemical property (Figure 2). The initial oxidation peak of Fc is 0.497 V. There is an oxidation peak at 0.810 V belonging to **TX-Ph2Cz**. According to the formula of $E_{HOMO}=-[E_{OX}-E_{Fc}+4.8]$,[21] the HOMO energy level of **TX-Ph2Cz** is −5.13 eV (Table 1). From the absorption spectra, the absorption edge (413 nm) is obtained and then the energy gap (E_g) *is* 3.00 eV. Correspondingly, the LUMO energy level (−2.13 eV) is calculated from the formula of $E_{LUMO}=E_{HOMO}+E_g$.

2.4 Photophysical properties

The UV-vis absorption and photoluminescence (PL) spectra in the different solvents (10^{-5} mol/L) with various polarities are shown in Figures 3a and 3b. With the increasing polarities, the absorption bands have no obvious change, indicating that it has a smaller ground state dipole moment. The absorption peaks before 350 nm are attributed to the π-π* transition of the carbazole groups, the absorption peaks at 350～375 nm belongs to the absorption of thioxanthone groups, and the absorption peaks at 375～410 nm are due to the intramolecular charge transfer transition from the donor to the acceptor. PL spectra (Figure 3b) shows that the emission peaks in different solvents are at about 420 nm belonging to the local excited (LE) state. It is found that emission bands in the solvents with high polarity have low intensity and another emission band at about 560 nm belongs to the charge transfer state. Moreover, the delay curve of **TX-Ph2Cz** in toluene solution is 1.11 ns. The PL emission at room temperature and phosphorescence emission at 77 K in 2-methyltetrahydrofuran solution are shown in Figure 3c. By calculation, the lowest singlet energy level (S_1) and lowest triplet energy level (T_1) are 3.04 and 2.67 eV, respectively, and the energy gap (ΔE_{ST}) between S_1 and T_1 is 0.37 eV indicating that the reverse intersystem crossing process cannot occur in the single-molecular state. The emission bands and intensity changes in different THF/H_2O (THF: tetrahydrofuran) solvents with the various volume content of water (0～99 vol%) are shown in Figure 3d. It can be seen that emission intensities increase with the increasing volume content of water and the emission bands have a 36 nm red-shift owing to the aggregation. The photographs of **TX-Ph2Cz** in the pure THF solution and THF/H_2O solution with 99% (volume fraction) water content are deep blue and sky blue, respectively. From the above results, it indicates that **TX-Ph2Cz** has an aggregation-induced enhanced emission (AIEE) property. Furthermore, **TX-Ph2Cz** has ns magnitude lifetime that shortens with the increasing water content. It indicates that in the relatively tight aggregation **TX-Ph2Cz** has rapid radiative transition channel for the singlet excitons. The emission band in the solid is 462 nm. In addition, PL spectrum in the pure film exhibits blue emission at 458 nm with a photoluminescence quantum yield (PLQY) of 1.74%.

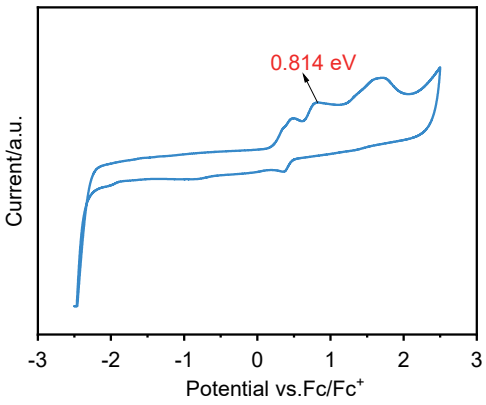

Figure 2 CV curve of **TX-Ph2Cz**

Table 1 Summary of thermal stability, electrochemical and photophysical properties

Compound	λ_{abs}[a]/nm	λ_{PL}/nm	T_d/℃	T_g/℃	HOMO/eV	LUMO/eV	τ[a]/ns	Φ_{PL}[b]/%	S_1/eV	T_1/eV	ΔE_{ST}/eV
TX-Ph2Cz	315, 339, 389	420[a]/458[b]	383	142	−5.13	−2.13	1.11	1.74	3.04	2.67	0.37

[a] In the toluene solution; [b] in the pure film.

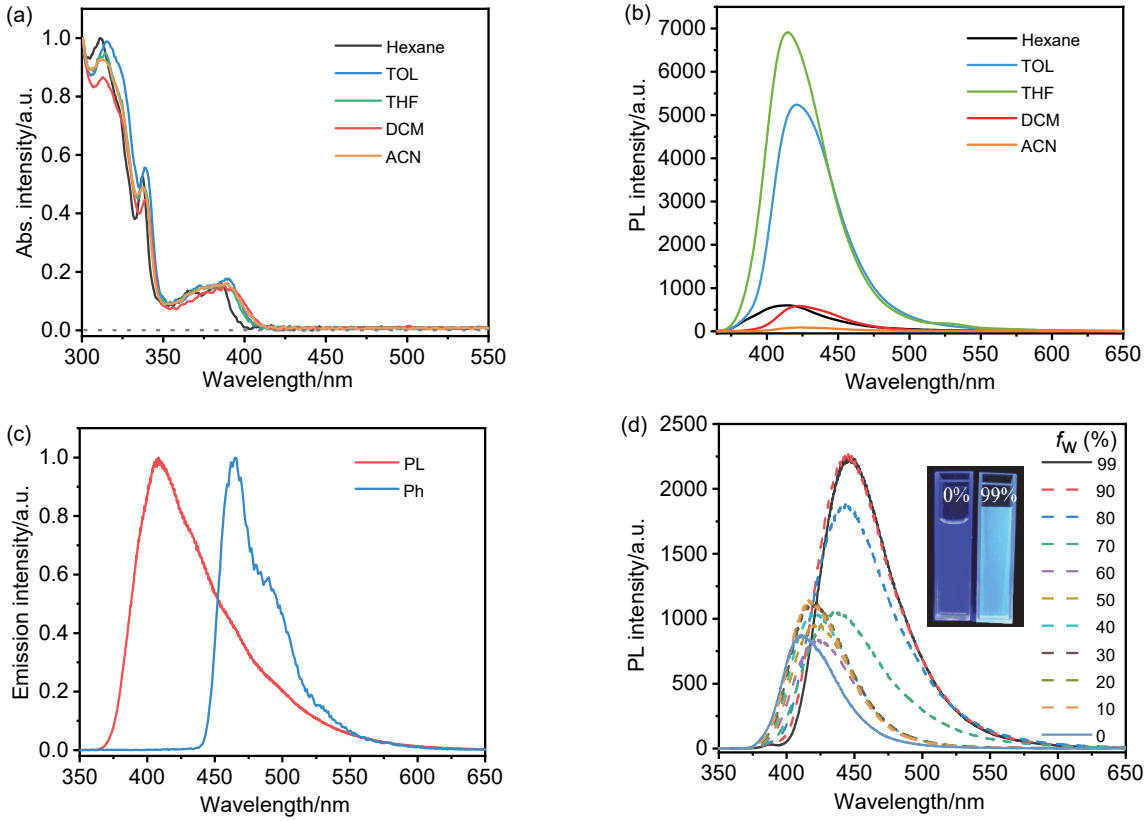

Figure 3 UV-vis absorption spectra (a) and PL spectra (b) of **TX-Ph2Cz** in different solvents (10^{-5} mol/L) with various polarities, PL spectrum and phosphorescence spectrum (c) at 77K in 2-methyltetrahydrofuran solution, and PL spectra (d) in the different THF/H_2O solution (inset: photographs of **TX-Ph2Cz**)

2.5 Theoretical calculation

In order to explore the excited-state characteristics, natural transition orbitals (NTOs) analysis of **TX-Ph2Cz** was investigated by density functional theory (DFT) calculation at B3LYP/6-31G* level and exported by Multiwfn 3.8 based on Gaussian output results (Figure 4). To ensure accuracy, 10 singlet and 10 triplet states were calculated. It is found that the ΔE_{ST} between S_1 and T_1 is 0.329 eV and no reverse intersystem crossing (RISC) process would appear. The overlap integrals ($\langle\Psi_h\Psi_e\rangle$) are 0.045 for S_1 and 0.650 for T_1 indicating the transitions of charge transfer state and locally excited (LE) state, respectively. Spin orbit coupling matrix elements (SOCME) were also calculated via the ORCA 5.0.1 package. Owing to the introduction of heteroatoms, spin-orbit coupling (SOC) value between S_1 and T_1 is relatively large that would enhance the ISC process. However, the SOC value between S_0 and T_1 is small indicating that high-effective radiative transition channel for triplet excitons is difficult. Thereby, serious quenching of singlet excitons and triplet excitons would appear and the luminous efficiency is relatively low.

2.6 Single crystal

Transparent single crystal of **TX-Ph2Cz** was obtained from the mixed solution of petroleum ether and dichloromethane (V ∶ V=1 ∶ 1) and characterized by single crystal X-ray diffraction (Figure 5). It belongs to a monoclinic system with the space group of $P21/n$ (CCDC: 2291912) and exhibits head-to-head cross parallel arrangement. The torsion angle between thioxanthone unit and benzene ring is 29.66° and the torsion angles between two carbazole groups and benzene ring are 47.02° and 38.72°, respectively. From the stacking of dimer, the crystal has many intramolecular interactions of C—H···O, C—H···π, π···π and C—H···H—C with the distances of 0.2341, 0.2810, 0.3329 and 0.2235 nm, respectively. It indicated that **TX-Ph2Cz** crystal has relatively tight arrangement and good rigid environment owing to the conjugated groups. It is also found that the interaction of π···π is originated from the conjugated thioxanthone unit and carbazole group, thereby effective intermolecular charge transfer state would present between the adjacent molecules.

2.7 Electroluminescent properties

To further investigate the electroluminescent properties, device configuration of ITO/MoO_3 (3 nm)/**TAPC** (40 nm)/**TCTA** (10 nm)/**CBP**: 3% and 100% (mass fraction) **TX-Ph2Cz** (20 nm)/**TmPyPB** (50 nm)/LiF (1 nm)/Al (100 nm) was adopted to prepare the evaporated OLEDs. Among the device (Figure 6a), 4-[1-[4-[bis(4-methylphenyl)amino]-phenyl]cyclohexyl]-*N*-(3-methylphenyl)-*N*-(4-methylphenyl)benzenamine (**TAPC**) and 4,4',4''-tris(carbazol-9-yl)-trienylamine (**TCTA**) were the hole transporting layer, 4,4'-bis(*N*-carbazolyl)-1,1'-biphenyl (**CBP**) acted as the

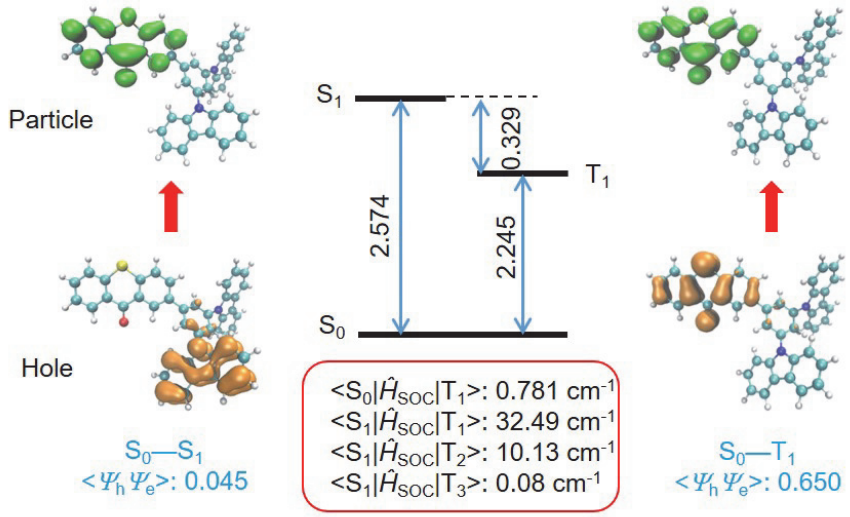

Figure 4 Natural transition orbitals (NTO) for $S_0 \rightarrow S_1$ and $S_0 \rightarrow T_1$ transitions, TD-DFT calculated energy levels, and corresponding spin-orbit coupling constants of **TX-Ph2Cz**

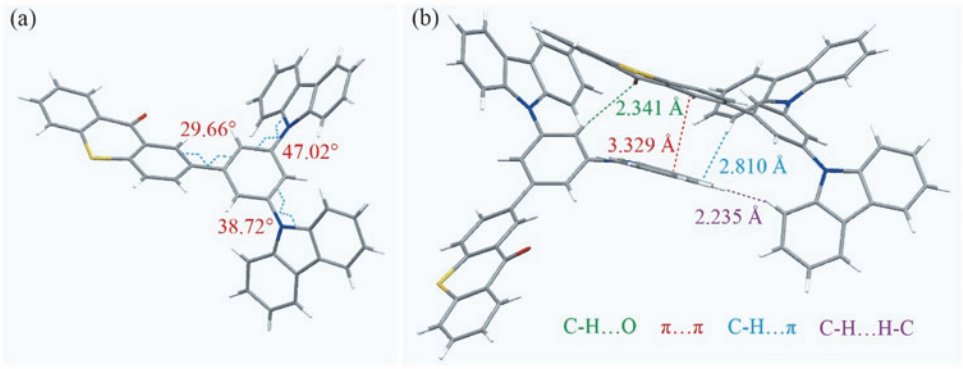

Figure 5 Molecular structure (a) and molecular stacking (b) of **TX-Ph2Cz**

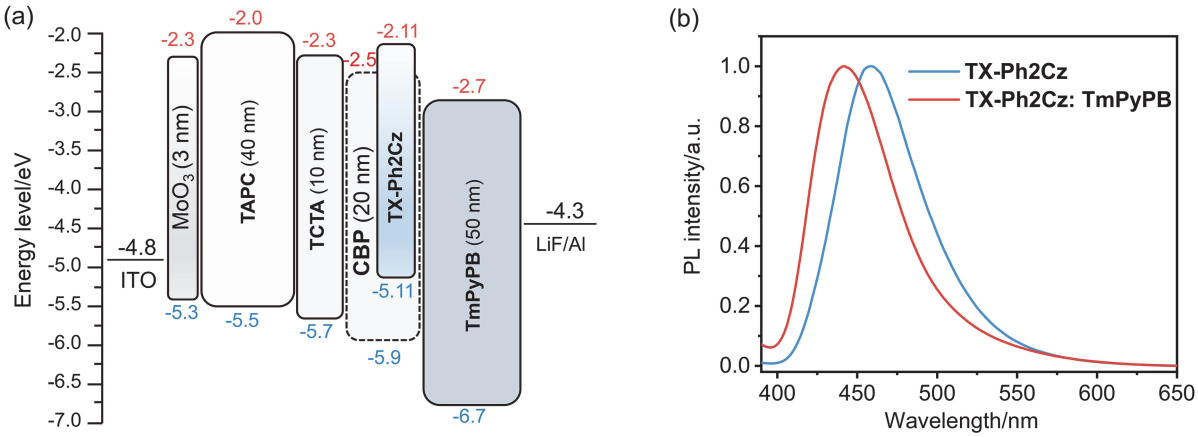

Figure 6 Device architecture and energy-level diagram of the functional materials (a) and PL spectra of the evaporated films (b)

host materials, 3,3'-[5'-[3-(3-pyridinyl)phenyl][1,1':3',1"-terphenyl]-3,3"-diyl]bispyridine (**TmPyPB**) was used as electron transporting layer. The energy levels in the device indicates that the exciplex emission between the **TX-Ph2Cz** and **TmPyPB** might be obtained. The PL spectra of the doped film were tested (Figure 6b). Regrettably, there is no exciplex emission. Amorphous pure film of **TX-Ph2Cz** has stronger intermolecular charge transfer state that causes a red-shift with the emission peaks of 458 nm in the PL spectra. From EL spectra (Figure 7a, Table 2), the doped device with 3% (mass fraction) **TX-Ph2Cz** exhibits a blue emission at 440 nm with the chromaticity co-

ordinate (CIE) of (0.169, 0.084) and a full width at half maximum (FWHM) of 35 nm. However, the non-doped device shows a yellow emission at 540 nm with the CIE of (0.340, 0.463) and FWHM of 60 nm. It can be explained as that the compound is electroactive and radical anions of oxygen maybe generate. At the same time, the interaction appears between the radical anions of oxygen and sulfur atom on the thioxanthone groups, thereby the excimer emission by molecular themselves is dominated in the non-doped devices.[22] Additionally, the turn-on voltages of **TX-Ph2Cz** are 4.5 and 4.6 V for non-doped and doped devices indicating the good carrier transporting ability. In the doped device, **TX-Ph2Cz** exhibits unsatisfactory EL performance with the maximum external quantum efficiency (EQE_{max}) of only 0.25%. In contrast, the non-doped device of **TX-Ph2Cz** shows a maximum EQE of 2.64%, a maximum current efficiency (CE) of 4.91 cd/A and a maximum power efficiency (PE) of 3.32 lm/W, which are higher than the literature.[18] The above results illustrates that the new excimer emission provides an effective radiative transition channel and further investigation is going on.

3 Conclusions

In summary, we designed and synthesized a novel Y-typed emitter (**TX-Ph2Cz**) using thioxanthone units as the acceptor and 9,9'-(1,3-phenylene)bis-9*H*-carbazole as the donor. Owing to the weak electron withdrawing ability of thioxanthone units, **TX-Ph2Cz** exhibits blue emission at about 420 nm in the diluted solution with small change in the different solvents with various polarities. In the different THF/H_2O solvents (1～99 vol%), the emission bands have a red shift of 36 nm. According to the single crystal, **TX-Ph2Cz** shows many intermolecular interaction (C—H···O, C—H···π, π···π, C—H···H—C) that is conducive to the intermolecular charge transfer state. Critically, **TX-Ph2Cz** exhibits blue emission (440 nm) in the doped device, but yellow emission (540 nm) in the non-doped device that originates from the excimer emission of **TX-Ph2Cz** themselves. Moreover, the maximum current efficiency and external quantum efficiency of non-doped device are 4.91 cd/A and 2.64%, respectively. It illustrates that excimer emission from the luminescent materials is

Table 2 Summary of electroluminescent properties for **TX-Ph2Cz**

Device	λ_{EL}/nm	V_{on}/V	L_{max}/(cd•m^{-2})	CE_{max}/(cd•A^{-1})	PE_{max}/(lm•W^{-1})	EQE_{max}/%	FWHM/nm	CIE (x, y)
TX-Ph2Cz	540	4.5	1445	4.91	3.32	2.64	60	(0.340, 0.463)
3% **TX-Ph2Cz**	440	4.6	224.8	0.19	0.12	0.25	35	(0.169, 0.084)

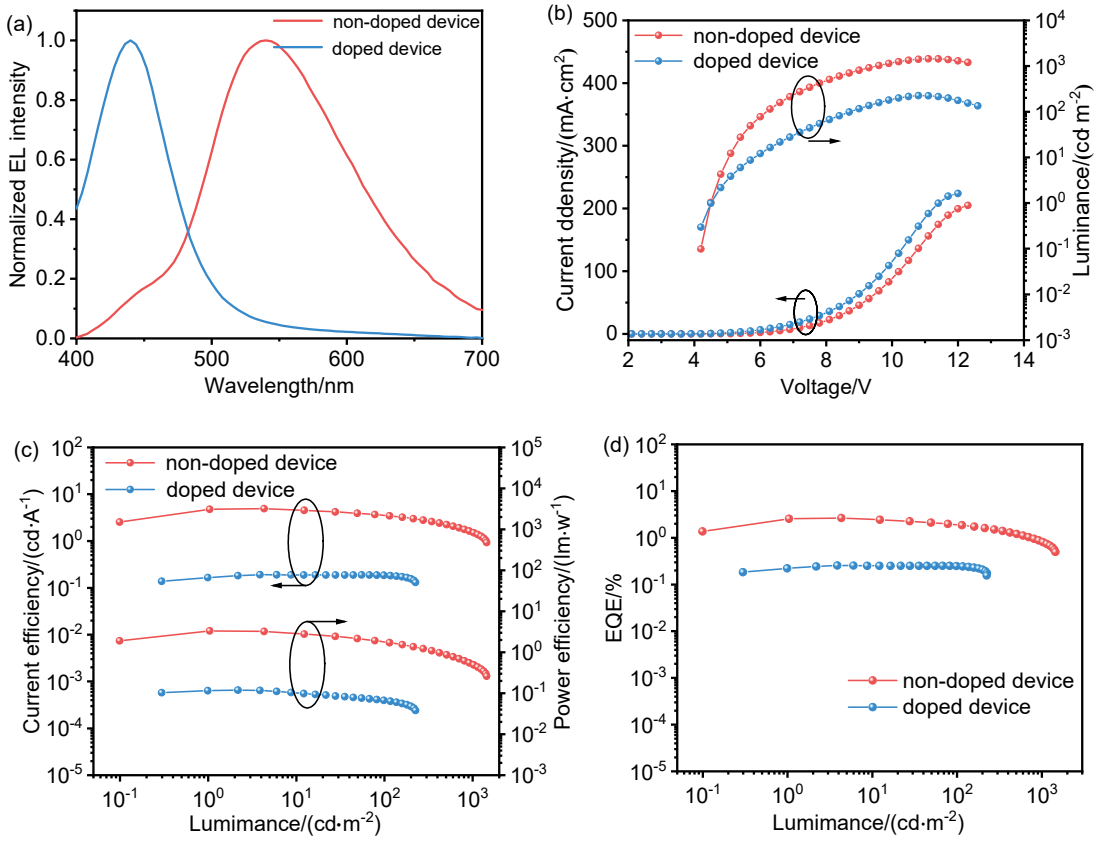

Figure 7 Electroluminescent properties of **TX-Ph2Cz**: EL spectra at 5 V (a), J-V-L curve (b), CE-L-PE curve (c) and EQE-L curve (d)

an effective strategy to improve the electroluminescent performance.

4 Experimental section

4.1 Instruments and reagents

^{1}H NMR and ^{13}C NMR spectra were recorded on a Bruker DRX 600 spectrometer at 400 and 101 MHz, respectively. Mass spectra were measured on a Bruker ultraflex MALDI-TOF/TOF spectrometry. The TGA curve was tested by a Netzsch TG 209F3 that heated from 100 ℃ to 700 ℃ with a temperature rate of 5 ℃/min under nitrogen atmosphere. The DSC curve was tested by a DSC Q2000 thermal analyzer, which was heated from 50 ℃ to 250 ℃ with a temperature rate of 10 ℃/min under nitrogen atmosphere, then rapidly cooled to room temperature and heated to 250 ℃. T_g was determined by the position of the inflection point in the second heating sweep curve. Cyclic voltammetry was measured by a CHI 660E electrochemical workstation. UV-vis spectra and fluorescence emission spectra were recorded by a Lambda Bio 40, a HORIBA FluoroMax-4 spectrophotometer and an Edinburgh FLS 980 spectrometer, respectively. X-ray single crystal diffraction was obtained on a Bruker D2 phaser X-ray diffractometer. The calculation of **TX-Ph2Cz** was studied from the density functional theory (DFT) using b3lyp functional with 6-31G(d) as the basic set through the Gaussian 09 program package. Electroluminescent devices were prepared under the vacuum degree of 5×10^{-5} Pa. Electroluminescence (EL) spectra were measured by the equipment of PR-655 spectrophotometer. The current density-voltage-luminance (J-V-L) characteristics were tested by the equipment of Keithley 2400 Source Meter and ST-900M Spot Brightness Meter. Except for specially stressed tests, general tests were recorded at room temperature.

4.2 Synthesis

4.2.1 Synthesis of 9,9'-(5-bromo-1,3-phenylene)bis(9*H*-carbazole) (**Ph2CzBr**)

Under nitrogen atmosphere, 9*H*-carbazole (3.34 g, 20 mmol), potassium *tert*-butoxide (2.24 g, 20 mmol) and dimethyl sulfoxide (20 mL) were added in the reaction bottle and stirred at 120 ℃ for 30 min, and then 1-bromo-3,5-difluorobenzene (1.93 g, 10 mmol) was added. The reaction mixture was stirred at 140 ℃ for 2 h. After cooling to the room temperature, the reaction mixture was extracted by chloroform and deionized water. Then, organic layer was dried, filtrated and evaporated in turn. The crude product was purified by column chromatography on silica gel with dichloromethane/petroleum ether as eluent. Finally, white powder of **Ph2CzBr** was obtained with 72% yield (3.51 g). ^{1}H NMR (400 MHz, Chloroform-d) δ: 8.15 (dt, J=7.7, 1.0 Hz, 4H), 7.87 (d, J=1.9 Hz, 2H), 7.80 (t, J=1.9 Hz, 1H), 7.55 (dt, J=8.3, 0.9 Hz, 4H), 7.47 (ddd, J=8.3, 7.1, 1.2 Hz, 4H), 7.33 (ddd, J=8.0, 7.1, 1.0 Hz, 4H). The data of ^{1}H NMR spectra is consistent with previously reported data (Ref. [23]).

4.2.2 Synthesis of 9,9'-(5-(4,4,5,5-tetramethyl-1,3,2-dioxaborolan-2-yl)-1,3-phenylene)bis(9*H*-carbazole) (**Ph2Cz-B**)

Under nitrogen atmosphere, **Ph2CzBr** (1 g, 2.05 mmol), 4,4,4',4',5,5,5',5'-octamethyl-2,2'-bi(1,3,2-dioxaborolane) (0.78 g, 3.075 mmol) and potassium acetate (0.603 g, 6.15 mmol) were dissolved in anhydrous 1,4-dioxane (15 mL). Soon afterwards, 1,1'-bis(diphenylphosphino)ferrocene]-dichloropalladium (**II**) (0.15 g, 0.205 mmol) was added into the reaction solution. The mixture was refluxed at 80 ℃ for 14 h. After cooling to room temperature, the reaction mixture was extracted, dried and evaporated. The crude product was purified by column chromatography on silica gel with ethyl acetate/petroleum ether as eluents. Finally, **Ph2Cz-B** was obtained as a white powder with a yield of 61% (0.67 g). ^{1}H NMR (400 MHz, Chloroform-d) δ: 8.15 (dt, J=7.8, 0.9 Hz, 4H), 8.12 (d, J=2.1 Hz, 2H), 7.88 (t, J=2.1 Hz, 1H), 7.52 (dt, J=8.3, 1.0 Hz, 4H), 7.45 (ddd, J=8.2, 7.0, 1.2 Hz, 4H), 7.31 (ddd, J=7.9, 7.1, 1.1 Hz, 4H), 1.37 (s, 12H). The data of ^{1}H NMR spectra is consistent with previously reported data (Ref. [24]).

4.2.3 Synthesis of 2-bromo-9*H*-thioxanthen-9-one (**TX-Br**)

2-Mercaptobenzoic acid (10 g, 65 mmol) was slowly added to a mixed solution of concentrated sulfuric acid (100 mL) and bromobenzene (14 mL, 134 mmol). The mixture became reddish-brown liquid, and then sulfur dioxide gas generated that must be removed by sodium hydroxide solution. The reaction solution was heated to 100 ℃ and kept for 3～5 h until the color was dark brown. After cooling to room temperature, the mixture was poured into ice water and yellow precipitate produced. The residue was purified by column chromatography on silica gel (dichloromethane/petroleum ether). Finally, yellow-green solid of **TX-Br** with 65% yield (12.3 g) was obtained. ^{1}H NMR (400 MHz, Chloroform-d) δ: 8.75 (d, J=2.2 Hz, 1H), 8.61 (dd, J=8.1, 1.4 Hz, 1H), 7.71 (dd, J=8.6, 2.2 Hz, 1H), 7.67～7.62 (m, 1H), 7.58 (dd, J=8.2, 1.3 Hz, 1H), 7.50 (ddd, J=8.2, 6.9, 1.3 Hz, 1H), 7.46 (d, J=8.6 Hz, 1H). The data of ^{1}H NMR spectra is consistent with previously reported data (Ref. [25]).

4.2.4 Synthesis of 2-(3,5-di(9*H*-carbazol-9-yl)phenyl)-9*H*-thioxanthen-9-one (**TX-Ph2Cz**)

Under nitrogen atmosphere, **TX-Br** (1 g, 3.43 mmol), **Ph2Cz-B** (1.93 g, 3.61 mmol), toluene (90 mL), and 2 mol/L aqueous potassium carbonate (5 mL) were added to a 250 mL flask, and then stirred at room temperature. The catalyst of tetrakis(triphenylphosphine)palladium (400 mg) was added and the reaction solution was slowly heated to 110 ℃ for 24 h. After cooling to room temperature, the mixture was extracted, dried, filtered and evaporated. The residue was purified by silica-gel column chromatography using dichloromethane/petroleum ether as eluents. **TX-Ph2Cz** was obtained as light green powder with 24.3% yield (0.515 g). ^{1}H NMR (400 MHz, Chloroform-d) δ: 8.97 (d, J=2.1 Hz, 1H), 8.64 (dd, J=8.1, 1.0 Hz, 1H), 8.18 (d,

J=7.7 Hz, 4H), 8.05 (d, J=1.9 Hz, 2H), 7.97 (dd, J=8.4, 2.2 Hz, 1H), 7.86 (t, J=1.8 Hz, 1H), 7.73 (d, J=8.4 Hz, 1H), 7.69～7.59 (m, 6H), 7.54～7.45 (m, 5H), 7.39～7.30 (m, 4H); ^{13}C NMR (100 MHz, Chloroform-d) δ: 179.67, 143.20, 140.58, 140.13, 137.42, 137.29, 136.93, 132.51, 130.79, 130.01, 129.66, 129.13, 128.09, 127.06, 126.60, 126.32, 126.11, 124.46, 124.31, 123.71, 120.53, 109.72. Anal. calcd for $C_{43}H_{26}N_2OS$: C 83.47, H 4.24, N 4.53, S 5.18; found C 84.03, H 4.19, N 4.35, S 5.17. HRMS calcd for $C_{43}H_{26}N_2OS$ 618.1766, found 618.1793.

Supporting Information ^{1}H NMR spectra of the intermediates **Ph2CzBr**, **Ph2Cz-B** and **TX-Br**; ^{1}H NMR, ^{13}C NMR, and HFMS spectra of final product **TX-Ph2Cz**; photograph of **TX-Ph2Cz** in different solvents; various PL intensities in the THF/H_2O solution with the increasing water fraction; transient PL decay curve in the different THF/H_2O solvents; molecular stacking; crystal data and structure refinement; transient PL delayed curves of **TX-Ph2Cz** in the doped and non-doped films; EL spectra of **TX-Ph2Cz** in non-doped and doped devices. The Supporting Information is available free of charge via the Internet at http://sioc-journal.cn/.

References

[1] Uoyama, H.; Goushi, K.; Shizu, K.; Nomura, H.; Adachi, C. *Nature* **2012**, *492*, 234.

[2] Lee, S. Y.; Yasuda, T.; Yang, Y. S.; Zhang, Q.; Adachi, C. *Angew. Chem., Int. Ed.* **2014**, *126*, 6520.

[3] Zhu, Y.; Qu, C.; Ye, J.; Xu, Y.; Zhang, Z.; Wang, Y. *ACS Appl. Mater. Interfaces* **2022**, **14**, 47971.

[4] Cao, X.; Zhang, D.; Zhang, S.; Tao, Y.; Huang, W. *J. Mater. Chem. C* **2017**, *5*, 7699.

[5] Kuang, Z.; He, G.; Song, H.; Wang, X.; Hu, Z.; Sun, H.; Wan, Y.; Guo, Q.; Xia, A. *J. Phys. Chem. C* **2018**, *122*, 3727.

[6] Wang, K.; Liu, W.; Zheng, C. J.; Shi, Y. Z.; Liang, K.; Zhang, M.; Ou, X. M.; Zhang, X. H. *J. Mater. Chem. C* **2017**, *5*, 4797.

[7] Ward, J. S.; Nobuyasu, R. S.; Batsanov, A. S.; Data, P.; Monkman, A. P.; Dias, F. B.; Bryce, M. R. *Chem. Commun.* **2016**, *52*, 2612.

[8] Zhang, W.; Song, H.; Kong, J.; Kuang, Z.; Li, M.; Guo, Q.; Chen, C.; Xia, A. *J. Phys. Chem. C* **2019**, *123*, 19322.

[9] Lee, J. H.; Cheng, S. H.; Yoo, S. J.; Shin, H.; Chang, J. H.; Wu, C. I.; Wong, K. T.; Kim, J. J. *Adv. Funct. Mater.* **2015**, *25*, 361.

[10] Park, Y. S.; Lee, S.; Kim, K. H.; Kim, S. Y.; Lee, J. H.; Kim, J. J. *Adv. Funct. Mater.* **2013**, *23*, 4914.

[11] Jankus, V.; Chiang, C. J.; Dias, F.; Monkman, A. P. *Adv. Mater.* **2013**, *25*, 1455.

[12] Jankus, V.; Data, P.; Graves, D.; McGuinness, C.; Santos, J.; Bryce, M. R.; Dias, F. B.; Monkman, A. P. *Adv. Funct. Mater.* **2015**, *24*, 6178.

[13] Kim, K. H.; Yoo, S. J.; Kim, J. J. *Chem. Mater.* **2016**, *28*, 1936.

[14] Moon, C. K.; Suzuki, K.; Shizu, K.; Adachi, C.; Kaji, H.; Kim, J. J. *Adv. Mater.* **2017**, *29*, 1606448.

[15] Nishimura, N.; Lin, Z.; Jinnai, K.; Kabe, R.; Adachi, C. *Adv. Funct. Mater.* **2020**, *30*, 2000795.

[16] Zhao, G.; Wang, B.; Liu, D.; Ma, D.; Chen, H.; Tian, W.; Ban, X.; Jiang, W.; Sun, Y. *Org. Electron.* **2021**, *99*, 106309.

[17] Jiang, S.; Lin, J.; Li, D.; Li, M.; He, Y.; Xie, W.; Chen, J.; Gan, Y.; Yang, G. X.; Yang, Z.; Li, W.; Su, S. J. *Chem. Eng. J.* **2023**, *452*, 139201.

[18] Yao, M.; Bian, B.; Wu, R.; Sun, K.; Tian, X.; Gong, T.; Liu, H.; Zhang, S. T.; Yang, B. *Org. Electron.* **2023**, *122*, 106905.

[19] Zhang, D. D.; Suzuki, K.; Song, X. Z.; Wada, Y.; Kubo, S.; Duan, L.; Kaji, H. *ACS Appl. Mater. Inter.* **2019**, *11*, 7192.

[20] Shi, Y. Z.; Wang, K.; Li, X.; Dai, G. L.; Liu, W.; Ke, K.; Zhang, M.; Tao, S. L.; Zheng, C. J.; Ou, X. M.; Zhang, X. H. *Angew. Chem., Int. Ed.* **2018**, *57*, 9480.

[21] Chuang, T. H.; Yang C. H.; Kao, P. C. *Inorg. Chem.* **2009**, 362, 5017.

[22] Sun, Y.; Shi, M.; Zhu, Y. N.; Perepichka, I. F.; Xing, X.; Liu, Y. M.; Yan, C. Y.; Meng, H. *ACS Appl. Mater. Interfaces* **2020**, *12*, 24156.

[23] Cho, Y. J.; Yook, K. S.; Lee, J. Y. *Adv. Mater.* **2014**, *26*, 4050.

[24] Wu, C.; Wu, Z.; Wang, B.; Li, X.; Zhao, N.; Hu, J.; Ma, D.; Wang, Q. *ACS Appl. Mater. Interfaces* **2017**, *9*, 32946.

[25] Yang, J.; Guo, Q.; Wang, J.; Ren, Z.; Chen, J.; Peng, Q.; Ma, D.; Li, Z. *Adv. Opt. Mater.* **2018**, *6*, 1800342.

(Lu, Y.)

